Implementation of an Optimization Method for Inverse Heat Conduction and Sensor Position Correction

R. Dalshad[1], N. Perakis[2], O. J. Haidn[2], M. Pfitzner[1]
1. Institute for Thermodynamics, Bundeswehr University Munich, 85577 Neubiberg, Germany
2. Chair of Turbomachinery and Flight Propulsion, Technical University of Munich, 85748 Garching, Germany

Introduction

Film cooling is an effective method in gas turbines to cool and protect the surface of components from hot gases. Generally, air is taken from the compressor and injected through holes along the walls of the combustion chamber and of the turbine blades. The air forms a protective layer between the component and the hot gas. However, the need and requirements for higher efficiency and thrust to weight ratio in modern gas turbines lead to designs that are more compact and at the same time operate at higher temperature and pressure conditions. The reduced size and the extreme conditions can have two effects. The combustion of the fuel may not be fully completed within the reduced length of the combustor, so that local fuel-rich products reach the turbine vanes. The residual fuel may react with the oxygen in the cooling air near the wall. Higher operating temperatures favors the chemical reactions additionally. Instead of cooling, heat is generated from the chemical reactions near the wall and it affects the thermal condition of the component.
Such secondary reactions are observed in Ultra Compact Combustors and investigated by Katta et al. [1]. The test bench in [1], which is described in detail by Evans [2], is operated at fuel-rich condition and air is injected in the test section to reproduce the secondary reaction. The test section is equipped with thermocouples stacks to measure the temperature. Each stack consists of two thermocouples to determine the heat flux. The authors reported on increase heat loads to the structure. However, the heat flux was only calculated at discrete positions. Perakis et al. [3] went a step further and combined experimental data and numerical simulations. They equipped test sections for rocket combustion investigations with multiple thermocouples (TC) in flow direction and perpendicular to the flow direction. The thermocouples were mainly located within the test section wall. Based on the measured temperatures and positions, known boundaries and material properties of the test section, they applied the inverse heat transfer methods to recalculate the temperature of the wall surface exposed to the combustion and determined the heat flux two-dimensionally. The optimization methods, namely Conjugate Gradient and Newton-Raphson, are described in detail by Özisik et al. [4].
Generally, heat conduction problems can be divided into direct and inverse problems. In direct problems, the thermal boundary conditions (heat flux or temperature) are given and its effect is calculated, while for inverse problems the boundary conditions are determined based on their effect. For some experimental setups, the measurement of temperature or heat flux at a specific boundary is technically not feasible, because of inaccessibility or thermal loads on the boundary exceed the limit of the sensors, such as thermocouples. Therefore, the thermocouples are placed at favorable locations, which are sensitive to the effects of the boundary and where access is granted. Based on the measured temperature data and the material properties, the heat flux on the unknown boundary can be calculated inversely. However, the inverse calculation is an iterative process and for long runtime experiments with high-frequency optimization, it tends to be time-consuming. Therefore improvements are required.
The objective of this work was the implementation of the inverse heat conduction (IHC) methods Newton Raphson and Conjugate Gradient Method [4] in LiveLink/COMSOL. To increase the efficiency and save optimization time, the Jacobian matrix was calculated once prior to the first time step and remained constant during the complete optimization process, as reported in [3]. Further, the thermocouple measurement is a contact-based technique and, depending on the sensitivity of the problem, minor errors in the positioning may have a major effect on the inverse calculated heat flux. Hence, the heat flux optimization was extended by a second optimization routine to correct the thermocouple positions iteratively. Both routines were coupled to each other, since the position variation resulted in a new heat flux optimization. The IHC method was applied to measurements of an in-house test bench. The experimental data were obtained by 11 thermocouples installed within a metal block, which was exposed to reactive near wall combustion of methane (CH4) and hydrogen (H2). The experimental runtime was over five hours. The optimization was realized in Matlab, while the direct problem was solved in COMSOL.

Test bench and data acquisition

The background and purpose of the IHT implementation is the thermal calculation of an in-house experimental work where near wall reactions are investigated. A gas generator provides oxygen-rich hot gas [5]. The combustion products were redirected to a water-cooled test section manufactured from Hastelloy C22, optical access was provided through fused silica windows from three sides. An isometric view of the test section is presented in Figure 1 (left). Holes of $0.4\ mm$ diameter and $30°$ angle were machined through the section wall where cold fuel (CH4 or H2) was injected. The fuel and the hot gas mixed and ignited. The auto-ignition depended on different factors such as mixture temperature, injection and main flow velocitiy, fuel type and injection angle. Due to the chemical reaction, the test section wall was subject to increased heat flux. 11 TCs of type K and $1\ mm$ diameter were implemented within the test section wall at the centerline as pictured in Figure 1 (right). The measured positions of the TCs are listed in Table 1. The TC holes were manufactured by erosion. The TC data were acquired by a National Instruments cRio (9045) with built-in calibration curves for thermoelectric voltage to temperature conversion. The sample rate was $2.85\ Hz$.
Each experiment consisted of a warm-up period, where the burner power was increased successively until the hot flow

temperature exceeded 1300 K and an average velocity of around 20 m/s was reached.

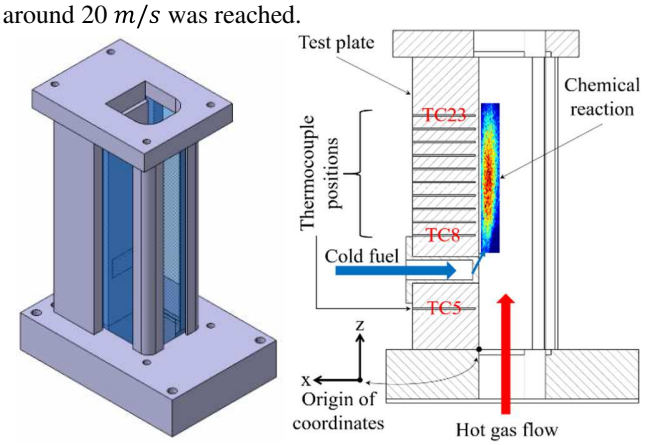

Figure 1: Isometric view (left) and cut view at the center line (right)

The flow temperature was measured by a thermocouple type B, while the velocity was calculated based on the supplied CH4 and air mass flows. Then, fuel was injected for a short period through the 5 nozzles and then turned off again. This injection procedure was repeated for different fuel velocities. The transient temperatures of three thermocouples are highlighted in Figure 2. Each spike in the curves represents one injection cycle. TC5 does not feature the spikes because it was not exposed to the injected fuel and the chemical reaction. Some injections are labeled for explanation purposes. The other, unmarked spikes were from different injected gases and mixtures.

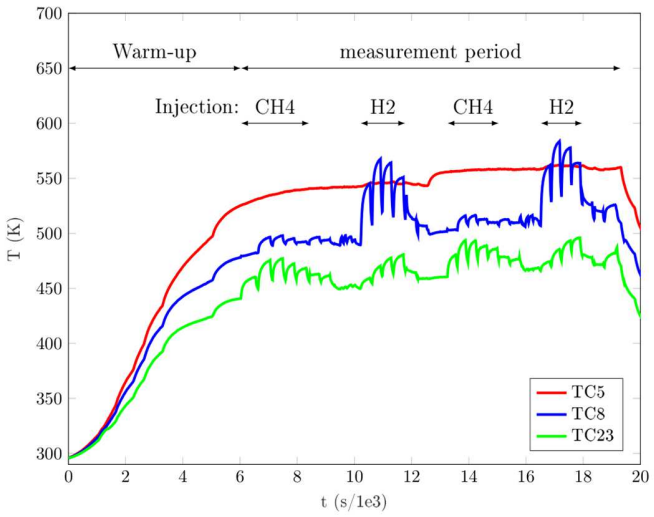

Figure 2: Transient temperature of selected TCs

Governing Equations for Inverse Heat Conduction

As mentioned before, the inverse method deals with problems where the boundary conditions are calculated based on their effect. A short description of the equations is presented in this section. For a detailed explanation, the authors refer to Özisik et al. [4]. In the current case, the temperature inside the plate was measured at positions specified in Table 1. However, the cause, which was the heat flux at the surface (x $=$ 0 mm), was unknown. For both methods discussed in this work, the aim was to find the heat flux on the surface and on the corresponding z-position such that the least square function S, also called objective function, was minimized:

$$S(\boldsymbol{P}) = [\boldsymbol{Y} - \boldsymbol{T}(\boldsymbol{P})]^T[\boldsymbol{Y} - \boldsymbol{T}(\boldsymbol{P})] \quad (1)$$

$\boldsymbol{Y}$ is the vector of n measured temperatures while $\boldsymbol{T}(\boldsymbol{P})$ is the vector of calculated temperatures depending on the unknown parameters $\boldsymbol{P}$. The latter is the heat flux applied on the surface. To minimize the least square function, the derivative of $S(\boldsymbol{P})$ with respect to $\boldsymbol{P}$ is set to zero.

$$\nabla S(\boldsymbol{P}) = -2\left[\frac{\partial \boldsymbol{T}^T(\boldsymbol{P})}{\partial \boldsymbol{P}}\right][\boldsymbol{Y} - \boldsymbol{T}(\boldsymbol{P})] = 0 \quad (2)$$

The transpose of the derivative of $\boldsymbol{T}$ with respect to $\boldsymbol{P}$ is called sensitivity or Jacobian matrix.

$$\boldsymbol{J}(\boldsymbol{P}) = \left[\frac{\partial \boldsymbol{T}^T(\boldsymbol{P})}{\partial \boldsymbol{P}}\right]^T \quad (3)$$

The elements of the Jacobian matrix, called sensitivity coefficients, are calculated by forward difference with an $\varepsilon = 10^{-5}$.

The iterative procedure for the Newton-Raphson (NR) uses the linearization of the estimated temperature by means of a Taylor expansion.

$$\boldsymbol{T}(\boldsymbol{P}) = \boldsymbol{T}(\boldsymbol{P}^k) + \boldsymbol{J}^k(\boldsymbol{P} - \boldsymbol{P}^k) \quad (4)$$

The superscript k indicates the iteration. Combining equations 2 and 4 leads to the next iterative expression for the estimated parameter vector $\boldsymbol{P}$.

$$\boldsymbol{P}^{k+1} = \boldsymbol{P}^k + (\boldsymbol{J}^k)^{-1}[\boldsymbol{Y} - \boldsymbol{T}(\boldsymbol{P}^k)] \quad (5)$$

The parameter $\boldsymbol{P}$ is estimated until the least square function achieves a stopping criterion.

The Conjugate Gradient method on the other hand minimizes the objective function based on the direction of descent and a calculated step size. The parameter for the next iteration is given as:

$$\boldsymbol{P}^{k+1} = \boldsymbol{P}^k - \beta^k \boldsymbol{d}^k \quad (6)$$

$\boldsymbol{d}$ is the direction of descent, while β is the step size. The direction of descent for the current iteration is chosen such that the angle between the direction of descent from the previous iteration and the negative gradient is less than 90°.

$$\boldsymbol{d}^k = \nabla S(\boldsymbol{P}^k) + \gamma^k \boldsymbol{d}^{k-1} \quad (7)$$

The conjugation coefficient γ is taken as the Fletcher-Reeves formulation with $\gamma^0 = 0$. Other expressions can be found in literature [4].

$$\gamma^k = \sum_{j=1}^{n}[\nabla S(\boldsymbol{P}^k)]_j^2 \Big/ \sum_{j=1}^{n}[\nabla S(\boldsymbol{P}^{k-1})]_j^2 \quad (8)$$

n is the number of parameters to optimize. The number of optimization parameters can be below, equal or above the number of measurement points. In this work, an equal number was set for a determined optimization problem. The search step size is derived from the objection function itself and defined as:

$$\beta^k = ([\boldsymbol{J}^k\boldsymbol{d}^k]^T[\boldsymbol{T}(\boldsymbol{P}^k) - \boldsymbol{Y}])/([\boldsymbol{J}^k\boldsymbol{d}^k]^T[\boldsymbol{J}^k\boldsymbol{d}^k]) \quad (9)$$

The nature of the investigated experiment needed a transient optimization process. Hence, the IHT was conducted for each point of time successively. The generic parameter vector P is in case of IHT the vector of specific heat fluxes $\dot{\boldsymbol{Q}}$. Means, $\boldsymbol{T}(\boldsymbol{P}) = \boldsymbol{T}(\dot{\boldsymbol{Q}})$ and $\boldsymbol{J}(\boldsymbol{P}) = \boldsymbol{J}(\dot{\boldsymbol{Q}})$. Both methods were implemented as described in the next section.

Implementation Routine for Inverse Heat Conduction

The inverse methods described in the previous section required an iterative procedure. Generally, the unknown parameter is estimated, a direct problem is solved and the objective function is evaluated. This process is carried out until a desired convergence is reached. A suitable choice for this optimization process is COMSOL in combination with Matlab/LiveLink.
First, a direct case of the heat conduction problem was built in COMSOL and the transient know boundary conditions were defined. Those consisted of the natural convection of the outer surfaces and the internal convective water-cooling. The mass flow and temperature of the water were measured. Since the test section is symmetrical to the xz-plane, only half of the test plate was considered to save computational time, as presented in Figure 3 left.

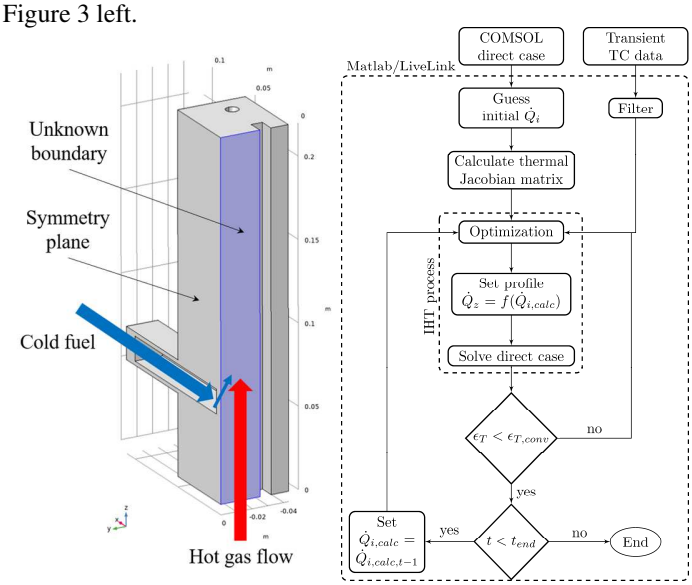

Figure 3: Direct problem case (left) and IHT process (right)

The unknown boundary, which was exposed to the hot gas and marked in Figure 3, was assigned a piecewise linear heat flux function in the z-direction with the same number of sections as the number of TC measurement points and constant extrapolation. The initial value of the heat flux was set to zero. Next, the direct case was loaded to Matlab/LiveLink alongside the transient TC data measured within the test section. The TC data were filtered to reduce the sample rate of $2.85\,Hz$ to $1/10\,Hz$. The filtering increased the simulation time step and reduced the number of transient optimization steps, which is beneficial due to the long run-time of the experiment. Further, the TC data noise was decreased by the filtering. At the same time, the information loss was minor. To determine the Jacobian matrix, $n+1$ simulations (n as number of optimized parameters) of the direct case were necessary. A major improvement in efficiency was the calculation of the Jacobian matrix only once at the beginning, as applied by Perakis et al. [3] and using it for every other time step as long as the positions of the TCs stayed unchanged. Thereafter, the optimization was performed and the vector of heat flux parameters $\dot{\boldsymbol{Q}}_{\boldsymbol{i,calc}}$ was determined and set for the heat flux function. Then, the direct case was solved and the convergence was checked. In case of convergence the next time step was started. A schematic description is illustrated in Figure 3 on the right side. This procedure was run until the complete run-time was simulated.

Implementation routine for inverse position correction

The TC in the test plate were hold in position using a spring mechanism and heat-conductive paste was used to enhance the contact between plate and TC. However, the heat transfer was particularly sensitive to the x-position of the TCs. Mostly, inaccuracies in the measurement of TC positions and imprecise positioning of TCs led to non-physical heat flux profiles. Therefore, the IHT method was extended by a second optimization routine, the inverse position correction (IPC), as pictured in Figure 4.

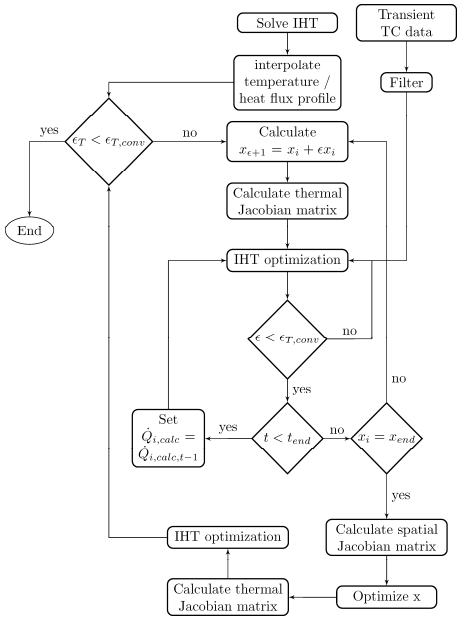

Figure 4: Inverse position correction process

The estimated parameters were in this case the x-positions of the TCs, while the temperatures or the heat fluxes were considered as given. At first, the IHC routine was performed with the initial measured TC positions for the warm-up period of the experiment. Next, a smoothed, physical profile of the surface temperature or heat flux was generated. If the surface temperature/heat flux and the fit diverged, a variation of each position successively was carried out with the final objective of a spatial Jacobian matrix and an IHT optimization. As specified in Figure 4 and mentioned in the previous section each position variation required a recalculation of the thermal Jacobian matrix, and solving of the transient IHC case. To determine the spatial Jacobian matrix of one x-optimization routine the direct case was run $n \cdot (n+1)$ times alongside the transient optimizations. Hence, the IPC was performed only for the short period of the experiment, which was the end of the warm-up period at around $\mathrm{t} = 5200\,s$. Then, the IHC was reran with the optimized/corrected x-positions.

Note that the area-specific heat flux is the product of heat transfer coefficient h and local temperature difference.

$$\dot{q} = h \cdot \Delta T \tag{10}$$

Further, the heat transfer coefficient is inversely proportional to the local distance as related by Nusselt correlations based on the boundary layer.

$$h \sim \frac{1}{(z+b)^n} \tag{11}$$

z is the axial distance in the direction of the main flow and b is a shift of the starting point of the boundary layer. n is considered $1/2$ for laminar and $1/5$ for turbulent flows [6]. Equation 11 indicates that the heat flux is inversely proportional to the distance. Hence, the heat flux in this work behave similarly during the warm-up period before the cold fuel injection.

Optimization Results

Both optimization methods showed the same efficiency and convergence behavior, therefore only the results of the NR method are demonstrated. The number of internal iterations of the IHT is presented in Figure 5.

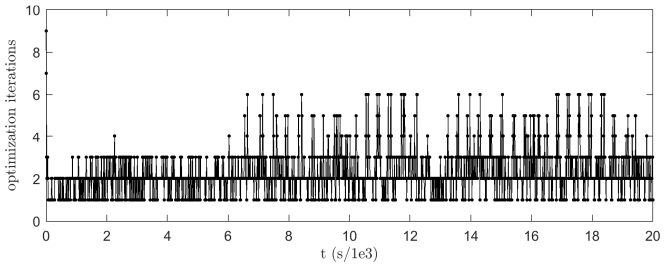

Figure 5: Number of internal iteration for the IHT

As mentioned earlier, each iteration loop required a direct simulation. The IHT took the highest number of iterations at the beginning, which was 9. Afterwards, only 3 iterations on average were necessary for convergence during the warm-up period (around $t = 6000\ s$). Between 4 and 6 iterations were needed for the injection period due to sudden thermal changes on the surface.

The top part of Figure 6 shows the transient temperature for some selected TCs, as well as the corresponding calculated heat fluxes. The measured and optimized temperatures with initial x-positions overlap predominantly, thus the discrepancy is illustrated in the middle part of Figure 6, where the maximum value is below $0.2\ K$. These discrepancies contribute to the objective function S. The convergence criteria for the objective function was set to $\epsilon_{T,conv} = 0.05\ K^2$, which was achieved and given in the bottom graph. The optimized results were in good agreement with the experimental data. The warm-up phase with slowly increasing thermal conditions as-well as the injection periods with sudden heat flux increase were reproduced by the optimization routine.

Considering the spatial temperature and the normal heat flux distribution, non-physical phenomena were observed, as pictured in Figure 7. The plots on top show the temperatures, while on bottom the normal heat flux is presented. The condition at $t = 5200\ s$ was during the warm-up period. During this time period, there is no reason for the local hot spots along the z-position. The 2D surfaces on the right row illustrate the effect of the correction of the TC positions. The temperature is decreasing monotonically from ca. $z = 100\ mm$ and the heat flux declines from the start of the surface, as expected. The hot spot in the temperature plots around $z = 60\ mm$ was caused by the injection chamber, as seen in Figure 3, because the water-cooling could not cool this region.

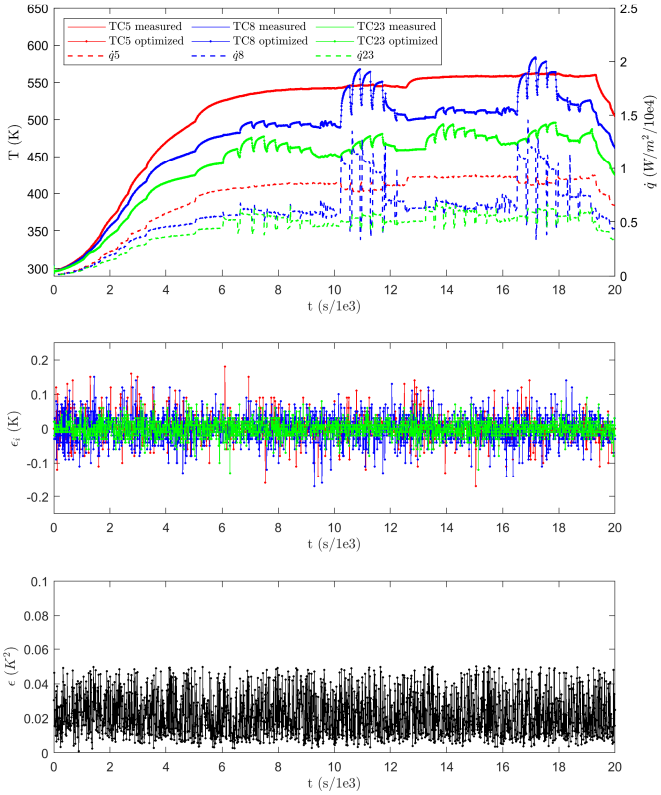

Figure 6: Measured and optimized temperatures (top), discrepancies ($TC_{measured} - TC_{optimized}$) (middle), objective value (bottom)

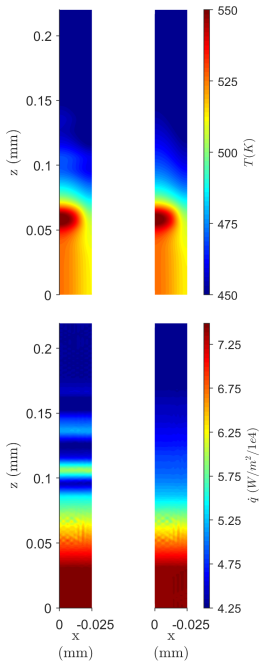

Figure 7: 2D temperature (top) and normal heat flux (bottom) at $t = 5200\ s$. On left uncorrected, on right corrected positions

A quantitative comparison of the spatial temperature and heat flux distribution is given in Figure 8. Up to z $= 31\,mm$ and above z $= 176\,mm$ the heat flux is constant because the constant value extrapolation was used. The temperature showed a wavy shape downstream of $z = 86\,mm$, while the heat flux exceeded a wavy form and resulted in a discontinuous zigzag shape, because it was more sensitive to the x-position. In a $10\,mm$ long z-range ($z = 96\,mm$ to $z = 106\,mm$) there was a fluctuation of more than $1.5e4\,W/m^2$.
Applying the IPC first for the temperature fitting and correction and later for the heat flux fitting and correction led to the continuous curves of Figure 8. The IPC in two-stages was necessary, because a one-stage correction based on the temperature did not correct the unphysical oscillations in the heat flux distribution entirely. Instead, a wavy shape was present due to the sensitivity of the heat flux. The second IPC based on the heat flux smoothed the curves finally.

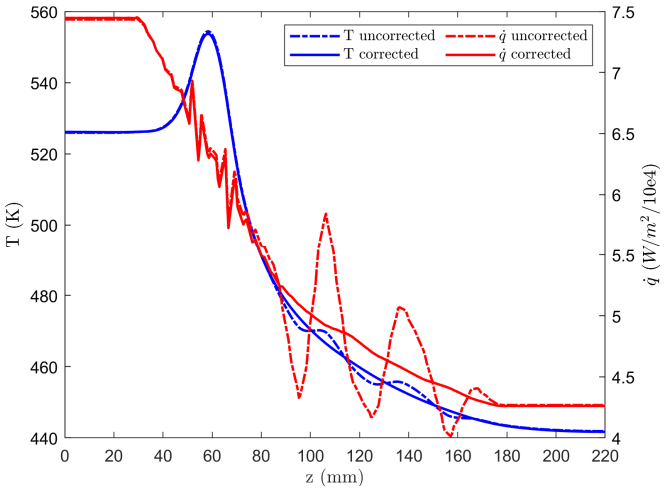

Figure 8: Temperature and normal heat flux along centerline for t $=$ 5200 s

The optimized x-positions for the smoothed curves of Figure 8 are listed in Table 1.

Table 1: TC position and correction

TC	z Position mm	x Position measured mm	x Position corrected mm	Difference mm
5	31	3.38	3.380	0
8	86	3.76	3.911	-0.151
11	96	4.09	4.361	-0.271
12	106	4.90	4.656	0.244
13	116	3.95	4.059	-0.109
16	126	3.26	3.556	-0.296
19	136	3.85	3.551	0.299
20	146	2.76	2.481	0.279
21	156	3.28	3.468	-0.188
22	166	2.89	2.936	-0.046
23	176	3.34	3.312	0.028

A maximum correction of 0.299 mm was determined. The results show the sensitivity of the problem to the TC position. Further, the small correction values were in the range of positioning error of thermocouples, since manual positioning for these dimensions were challenging. For the IPC, TC5 was not considered.
The optimization runs and the COMSOL direct simulations were performed on a 64-bit desktop computer with 4 cores @3.50 GHz and 64 GB of RAM. The IHT process with 11 parameters took around 40 h for 2000 optimization loops (20000 s of experimental time), while each position correction routine (temperature and heat flux based) required 16 h of calculation. Thereafter, the IHT was rerun with corrected positions. For the direct case, a fine mesh with local refinement on the unknown surface with around 38000 elements was generated.

Conclusions

Inverse heat transfer methods were successfully implemented in LiveLink/COMSOL to validate 1D thermocouple measurements of an in-house test-bench. Data of long run-time experiments were optimized for multiple parameters in an acceptable time span by means of single determination of the Jacobian matrix. Further, another optimization routine was implemented to correct inaccuracies in positioning of thermocouple. This method was applied twice for corrections based on temperature and heat flux profiles. The temperature and heat flux profiles were smoothed by optimizing the position of the thermocouples.
Other optimization methods, such as the Levenberg-Marquardt method, can also be implemented. It introduces a dumping factor which is adjusted depending on the convergence behavior. The method may lead faster to convergence. In the current work, the heat flux profile is assumed to be constant in the normal direction parallel to the surface (y-direction). However, thermocouples in y-direction are also installed. For the next step, a 2D optimization is sought.

References

1. V. R. Katta et al., On flames established with air jet in cross flow of fuel-rich combustion, *Fuel*, **150**, 360-369 (2015)
2. Dave S. Evans, The Impact of Heat Release in Turbine Film Cooling, *Thesis*, Air Force Institute of Technology, Ohio, 2008
3. N. Perakis, O. J. Haidn, Inverse heat transfer method applied to capacitively cooled rocket thrust chambers, *International Journal of Heat and Mass Transfer*, **131**, 150-166 (2019)
4. M. N. Özisik, H. R. B. Orlande, Inverse Heat Transfer, Fundamentals and Applications, Taylor & Francis, 2000
5. R. Dalshad et al., Experimental investigation of auto-ignition in non-premixed gaseous CH4/hot air cross section, *29. Deutscher Flammentag*, Bochum, 17.-18. September 2019
6. COMSOL Multiphyiscs® v5.5. www.comsol.com. COMSOL AB, Stockholm, Sweden.